

SIMULATION OF THE SOFTWARE RADIO MEASUREMENT OF EARTH ATMOSPHERE'S REFRACTIVE INDICES

ELEC 417

July 30th, 2017

Duc Huynh
V00789814



University
of Victoria



Acknowledgment

I would like to thank everyone involved in this project for their contributions in helping me reach my project goals. I would like to thank Dr. Peter Driessen for being my project supervisor and assisting me with any questions and problems that I encountered. Also, the ELEC517 Ionosphere Measuring team for providing practical measurements to verify my simulation program.

Contents

Executive Summary	Error! Bookmark not defined.
I Introduction	1
II Objectives.....	1
III Literature Survey.....	1
IV Design Methodology & Analysis.....	5
V Design & Prototype	7
VI Testing & Validation	8
VII Conclusion & Recommendations	11
References.....	12

I Introduction

The UViip team in UVic is constructing an atmosphere imaging device to investigate its ability to measure the Earth atmosphere's refractive indices for use to help monitor climate change. To verify the measurement results, it is essential to also construct a software simulation of the Earth's atmosphere response to the sweep signal that were sent. The method is based upon the synchronous measurement of the time taken for a radio wave to travel from the source, via the ionosphere to arrive at the receiving antenna at known positions from the radio wave source. The method provides information on the propagation of the radio wave through the Earth's atmosphere, which is a function of the refractive indices of its multiple layers.

II Objectives

- To analyze the radio HF wave propagation through the ionosphere
- To verify the ionospheric sounders made by the UViip team
- To demonstrate the Matlab coding technique that had been developed in the ELEC417 course

III Literature Survey

The formation of the Ionosphere depends on the solar radiation, by interacting with and removing electrons from different gases. Different wavelengths of solar electromagnetic energy, in the ultraviolet and X-ray parts of the spectrum, ionize different component gases in the atmosphere. Below figure shows the relationships between gas density, radiation intensity, and ionization.

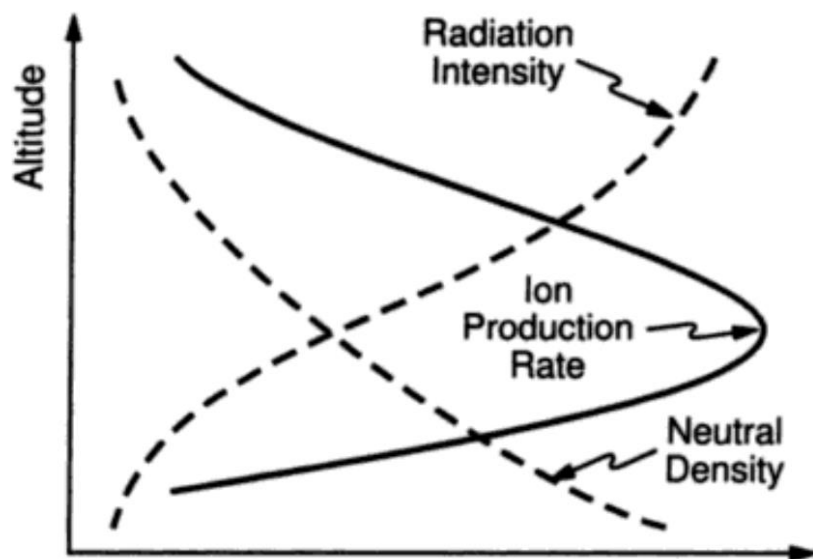


Figure 1 Relative Gas Density, Radiation Intensity, and Ionization Production Rate

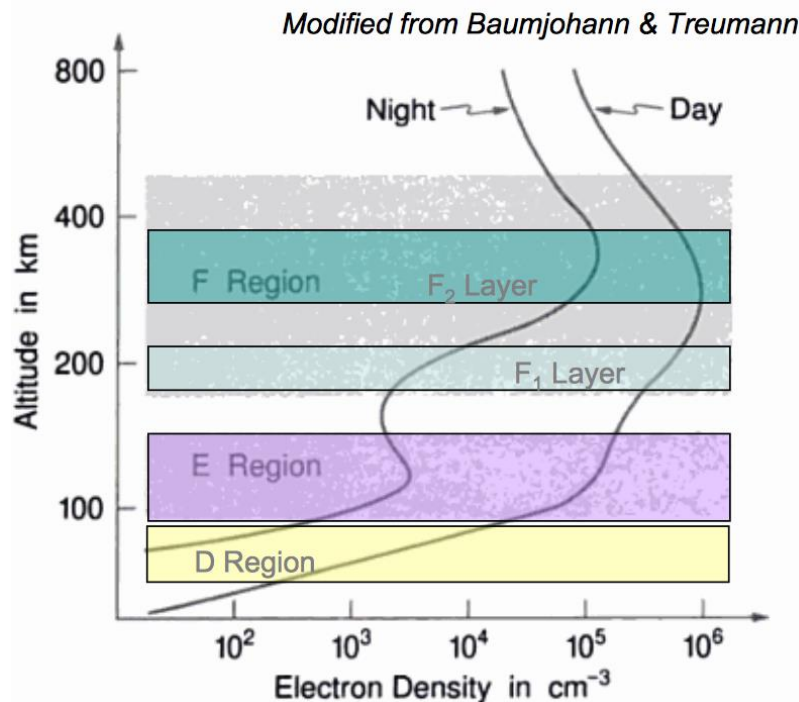
When a radio wave reaches the ionosphere, the electric field in the wave forces the electrons in the ionosphere to oscillate at the same radio wave's frequency. The oscillation may recombine, losing the radio energy, or re-radiate the original wave energy. Total refraction is expected when recombination is less than the radio frequency, and electron density in the ionosphere is large.

Ionization exists over the entire ionosphere and is varied with altitude. However, only the peaks in level may be considered as the different layers or regions of the ionosphere. The regions are known as D, E, and F (F1 and F2) regions (C layer is not considered here for its low level of ionization, thus no impact on radio waves).

The lowest layer, at altitudes of 50 to 80 km is the D layer. This layer acts as an attenuator, especially at low frequencies. The attenuation varies as the inverse square of the frequency, preventing low frequency signals from reaching to the higher layers. As frequency increases (meaning shorter wavelength), collisions between free electrons and gas molecules decrease. Thus, low frequency signals are attenuated more than the higher frequencies. The D layer disappears at night.

Next is the region E (100 to 125 km) and F (above 130 km). At night, layer F1 and F2 merge back into one layer and typically at around 250 to 300 km. Similar to layer D, signals entering E and F layers cause free electron to vibrate. However, the air density here is lower and there are fewer collisions. Rather than colliding with gas molecules and lost energy, the electrons tend to re-radiate the signal. Electron density is increased as the signal traveled further into the layer. The signal is refracted away from the area of higher electron density; the refraction coefficient is large enough that at HF, signals can be bend and send back toward Earth (reflection).

Depicting below is the typical electron distribution in the ionosphere, following with the refraction of the signal entering an ionized region.



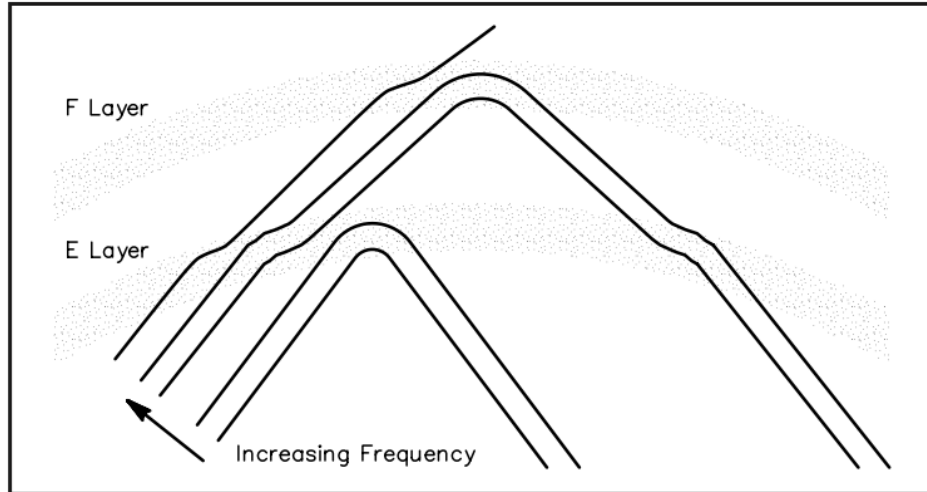


Figure 3 Refraction of Radio Wave Signal Entering an Ionized Region

A popular method of HF channel modeling was proposed by Watterson et. al. [4] in 1970. The Watterson channel model practically valid for a bandwidth up to one fourth of the reciprocal of the effective time spreads on the ionospheric components. Assuming a stationary model for the HF channel, the transmitted signal is fed into an ideal tapped delay line (TDL), and "is delivered at several taps with adjustable delays, one for each resolvable ionospheric modal component." Amplitude and phase of the delayed signal are modulated by a baseband tap-gain function, and then these components are summed to generate the output signal. Three hypotheses are made to specify the tap gain function: Each tap gain function is a complex Gaussian process that produces Rayleigh fading (figure 4); the tap gain functions are independent; each tap gain function has a spectrum that in general is the sum of two Gaussian functions. The channel model is illustrated in figure 5 below.

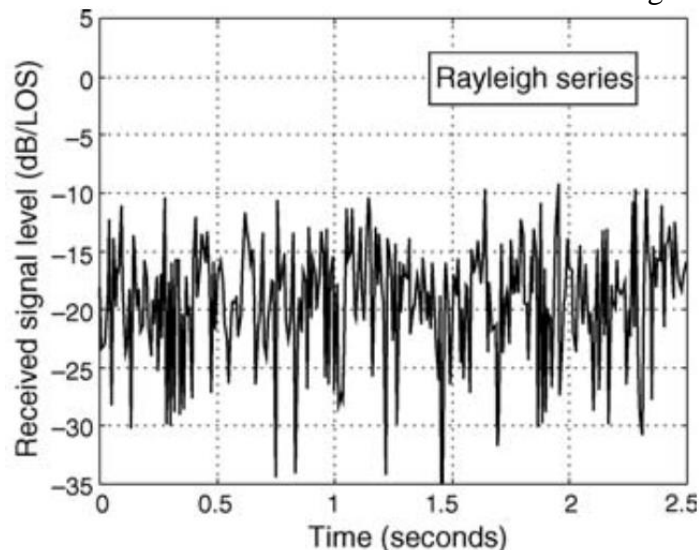


Figure 4 Rayleigh Series

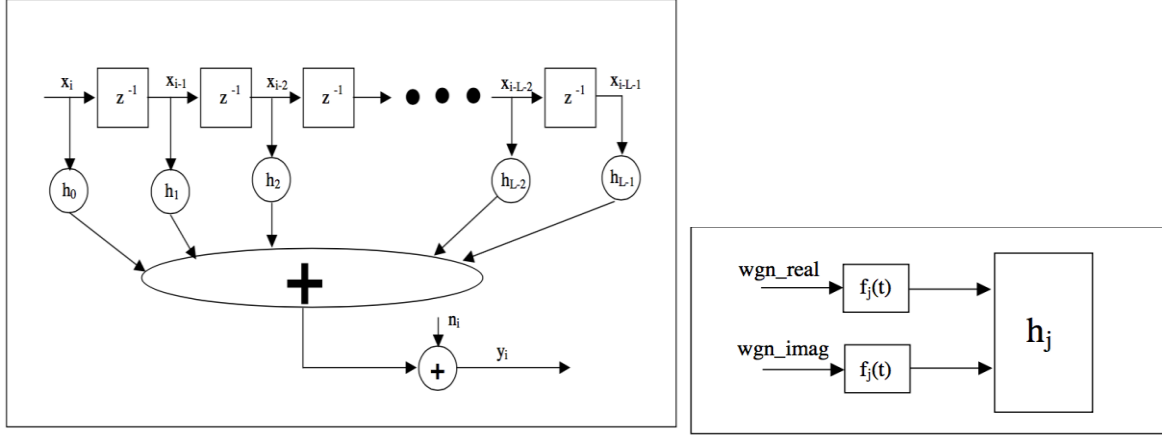


Figure 5 HF Channel Model

In the above figure, the time-varying taps (h_j) are generated by filtering complex WGN through filters whose frequency-domain power spectra have a Gaussian shape. The Doppler spread (d_j) is incorporated into the filter by setting the standard deviation (σ_j) of each Gaussian-shaped power spectrum equal to $d_j/2$. The amplitude of the tap in frequency-domain (i.e. $|H_j(f)|$) and the time-domain filter taps (generated by computing its inverse Fourier transform) are given by:

$$|H_j(f)|^2 = \frac{e^{-2f^2/d_j^2}}{\sqrt{\frac{\pi d_j^2}{2}}}; \quad -\infty < f < \infty \quad (1)$$

$$f_j(t) = \sqrt{2}e^{-\pi^2 t^2 d_j^2}; \quad -\infty < t < \infty \quad (2)$$

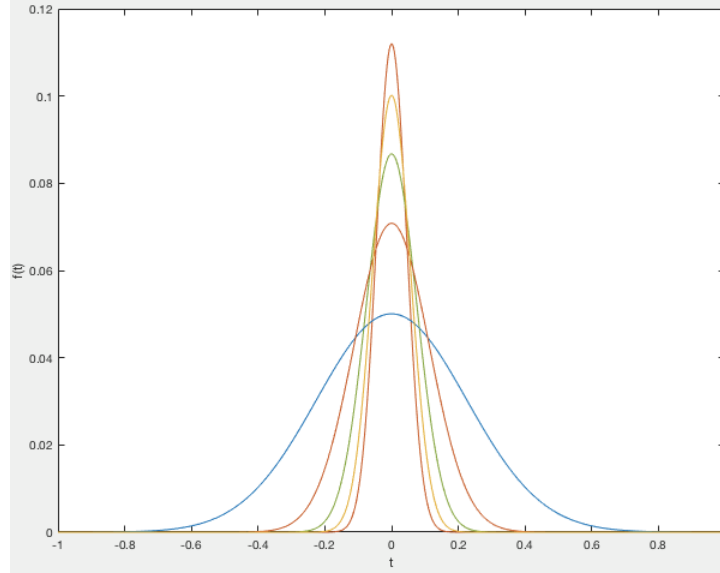


Figure 6 Time Domain Filter Taps

Next, a wide sense stationary-uncorrelated scattering (WWSUS) channel is studied in terms of its amplitude and phase responses.

As the frequency separation between two transmitted signals increased, the fading behavior at one of the frequencies is uncorrelated to the other. The correlation of these two frequencies depends on the time spreading of the dispersion of path lengths and associated

powers. Signals of larger bandwidths will be distorted. This property is known as frequency selective fading. The minimum bandwidth over which magnitude of the frequency correlation function is larger than half of its maximum value is called channel's coherence bandwidth. The time period, over which the magnitude of the spaced-time correlation function is at least half its maximum value is called coherence time. Channel can be classified by comparing its symbol duration (T_s) and signal bandwidth (B) with the coherence time and coherence bandwidth

- If $T_c \ll T_s$, channel varies during the transmission of a single symbol, and the received signal shows a strong time-variant behavior.
- If $T_c \gg T_s$, channel shows a time-invariant behavior, and considered constant over the transmission of a symbol time.
- If $B_c \ll B$, channel transfer function changes over the signal bandwidth B , and channel shows the frequency-selective behavior. Channel of this type is called wideband channel.
- If $B_c \gg B$, channel transfer function can be considered constant over the signal bandwidth. Channel is called narrowband channel

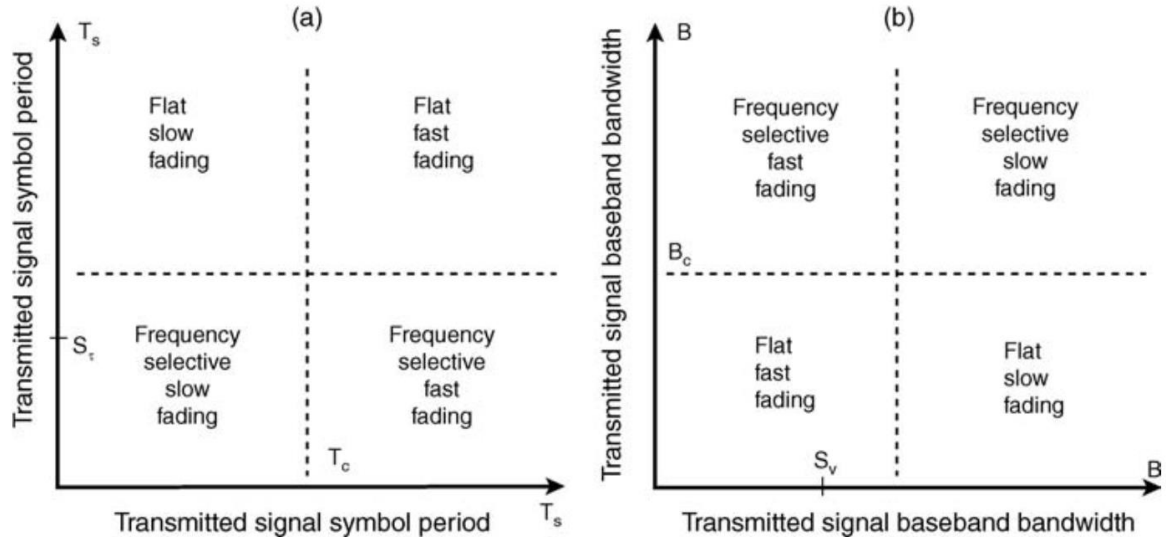


Figure 7 Classification of Channel with Respect to Symbol Period and Signal Bandwidth

IV Design Methodology & Analysis

In the following section, the methodology of simulating the HF propagation through the ionosphere is discussed. The simulating scenario is explained; steps to derive channel impulse response and frequency response are shown mathematically.

To simulate the propagation of HF signals through the ionosphere, we used the multiple point-scatterer model for synthesizing the signal's time variations, at or in the neighborhood of the carrier. The channel model of interest is the wideband channel. The simulation will show the selectivity of the channel (in the frequency domain), as well as the time selectivity (fading) of the channel.

The relationship between the transmitted passband signal, and its associated complex envelope representation is given by

$$x_{RF}(t) = Re[x_{CE}(t) \exp(j2\pi f_0 t)] \quad (3)$$

And the received signal is given by

$$y_{CE}(t) = \sum_{i=1}^N \tilde{a}_i \exp\{-j2\pi f_0[\tau_i + \tau_i(t)]\} * x_{CE}\{t - [\tau_i + \tau_i(t)]\} \quad (4)$$

Hence, the time-varying impulse response is determined by

$$h_{CE}(t, \tau) = \sum_{i=1}^N \tilde{a}_i \exp\{-j2\pi f_0[\tau_i + \tau_i(t)]\} * \delta\{t - [\tau_i + \tau_i(t)]\} \quad (5)$$

Time-varying frequency response is

$$T_{CE}(t, f) = \sum_{i=1}^N \tilde{a}_i \exp\{-j2\pi(f + f_0)\} [\tau_i + \tau_i(t)] \quad (6)$$

where \tilde{a}_i represents the magnitude and phase of the contribution from scatterer i

τ_i represents the propagation time (delay) and is equal to $d_i(t)/c$

c is the speed of light

Since the channel is time-variant, the impulse response is also a time-varying function. The relation between the complex envelope at the receiver, $y(t)$, and the input, $x(t)$ is defined as the convolution integral of

$$y(t) = \int_{-\infty}^{\infty} x(t - \tau)h(t, \tau)d\tau$$

where $h(t, \tau)$ is the time-varying impulse response of the channel

τ is the delay variable

The physical representation of the channel can be expressed in the form of the TDL (figure 5) as a summation

$$y(t) = \Delta\tau \sum_{-\infty}^{\infty} x(t - m\Delta\tau)h(t, m\Delta\tau)$$

Channel output $y(t)$ can also be represented by using the time-varying transfer function $T(t, f)$ as

$$y(t) = \int_{-\infty}^{\infty} X(f)T(f, t) \exp(j2\pi ft) df$$

where $T(t, f)$ is the Fourier transform of $h(t, \tau)$ with respect to variable τ

Other representations of the channel are as followed:

$$Y(f) = \Delta\vartheta \sum_{m=1}^n X(f - m\Delta\vartheta)H(f - m\Delta\vartheta, m\Delta\vartheta)$$

$$y(t) = \iint_{-\infty}^{\infty} x(t - \tau)S(\tau, \vartheta) \exp(j2\pi\vartheta t) d\vartheta d\tau$$

where $S(\tau, \vartheta)$ is the scattering function of the channel

The relationship between $h(t, \tau)$, $T(f, t)$, $H(f, \vartheta)$ and $S(\tau, \vartheta)$ is depicted in figure 8

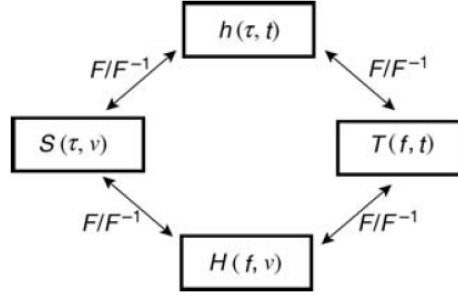


Figure 8 Relations between the four deterministic time-varying channel function

V Design & Prototype

Differing in its ion density at different heights complicates the refraction and reflection in different ionosphere layers. Furthermore, the multiple hops make simulating the HF propagation even more complicating. Hence, to simplify the scenario, the simulation involved three hypotheses:

- The reflection happens only at the ionosphere regions, no reflection is observed in the transition between two layers
- There is only one hop for each reflection ray, each hop is determined by a scatterer point of the ionosphere region, as demonstrated in figure 3
- Rate of reflection increase as altitude increase. In other words, layer D has least reflection, then comes layer E, and at F1, F2, most reflection is observed.

Three mains sub-functions of the simulations are: Propagation Scenario, Results Calculation, and Results Plotting.

The Propagation Scenario is described as followed. A sweep of LFM from 3.5kHz to 4kHz is transmitted at (0;0), through the ionosphere reflection, and to be received by an antenna at 5 km away on the x-axis. Note that the LFM is contained in a HF wave at frequency $f_0=5\text{MHz}$. The ionosphere layers are described by the scatterers with the following parameters. The altitude and thickness of the layer are defined in km as $\bar{A}\text{LayerAltitude}$, and $\bar{A}\text{Thick}$, respectively (with $\bar{A}=D,E,F1,F2$ is the layer name). $\bar{A}\text{Elec}$ ($\times 10^3 \text{ cm}^{-3}$) defined the electron density of the \bar{A} layer. The following parameters are applied in the simulation

Table 1 Simulation Parameter

Layer	Altitude (km)	Thickness (km)	Electron Density (%)
D	90	0.1	1
E	120	20	5
F1	220	20	40
F2	350	30	54

The Result Calculation steps are:

- Calculate the distance from the transmitter to the scatterer and then to the receiver
- \tilde{a}_i is determined by the following equations to ensure the validity of the link budget

$$2\sigma^2 = \sum_{i=1}^N a_i^2 = Na^2 \quad (7)$$

$$a_i = \frac{\frac{\sqrt{\sigma_i}}{d_{i-1}d_{i-2}}}{1/d_0}$$

- The impulse response of the channel is then determined and by equation (5) above with

$$2\pi(f_0)\tau_i(t) = 2\pi(f_0)\frac{d_i(t)}{c} = k_c d_i(t)$$

- Similarly, the time-varying frequency response of the channel is determined by equation (6)
- As shown in the Analysis section, the time-vary impulse response of the channel is derived by taking the inverse Fourier transform of the time-varying frequency response.

Plots of the scatterer scenario, time-varying impulse response, and its absolute value, as well as time-varying frequency response are depicted.

VI Testing & Validation

The scattering scenario is plotted as in figure 9, then the channel responses are plotted as followed

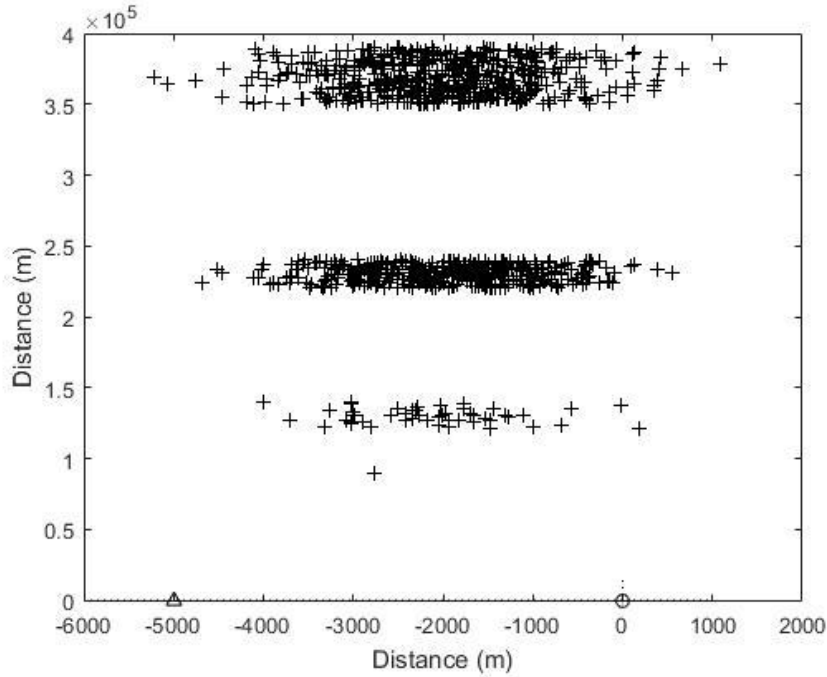


Figure 9 Scattering Scenario of the Ionosphere

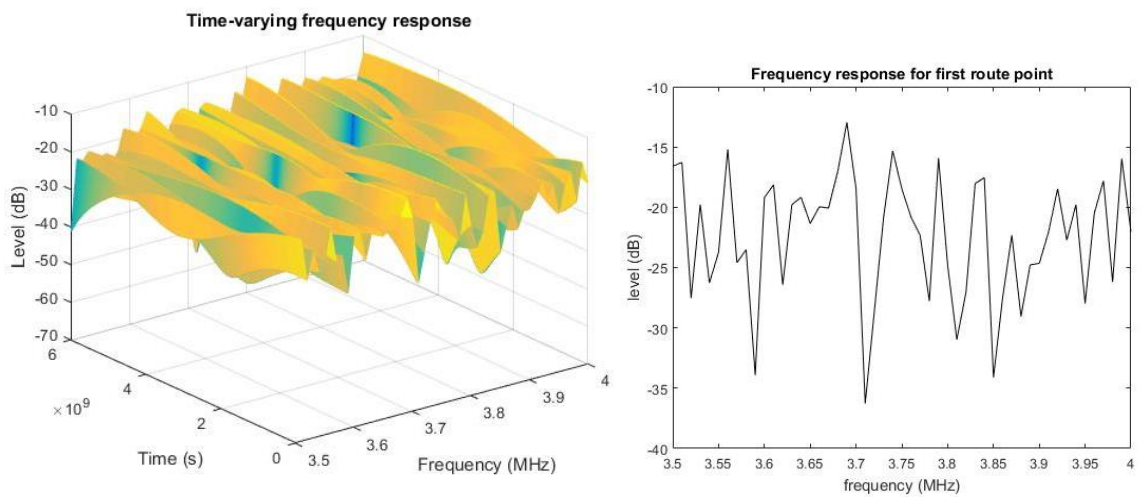


Figure 10 Time-Varying Frequency Response

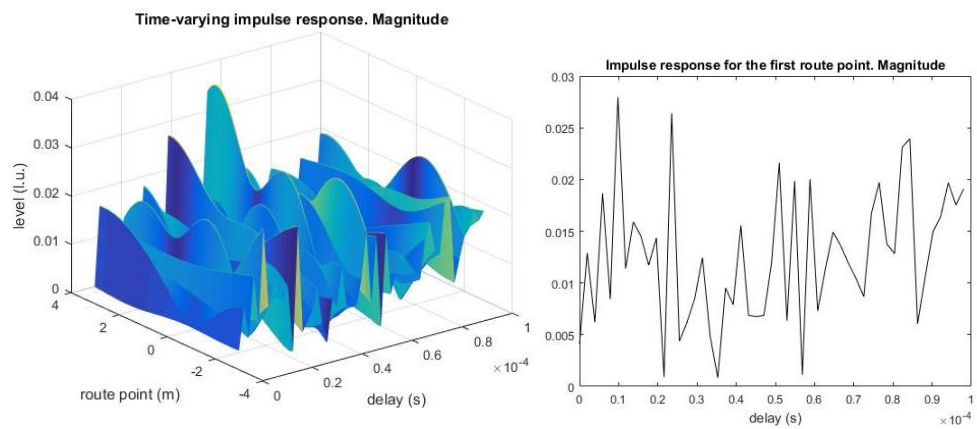


Figure 11 Time-Varying Impulse Response

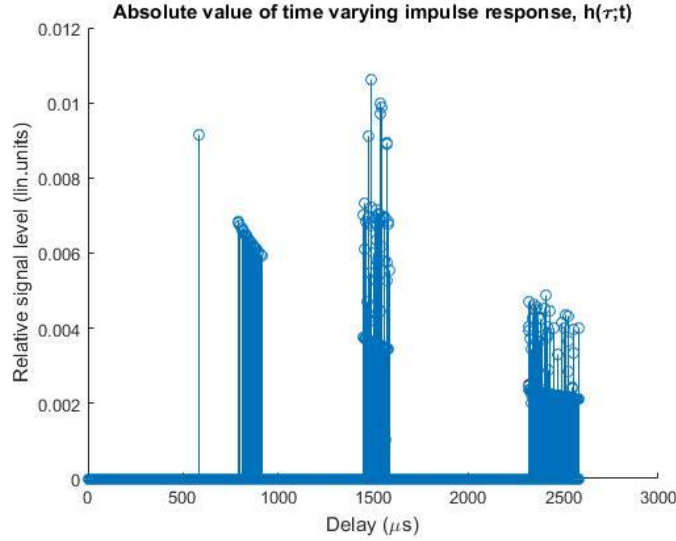


Figure 122 Absolute Value of Time-Varying Impulse Response

Using the above absolute value of the time-varying impulse response, the altitude and thickness of the ionosphere can be determined.

For example, the first stem of the impulse response is shown at about 600us, and is a very thin stem. This is the ionosphere reflection at daytime of D layer, its altitude can be calculated by $h = t * \frac{c}{2} = 600 \text{ us} * 3 * \frac{10^8}{2} = 90\text{km}$.

Similarly, the second set of impulse response is at about 780us, and having a spread for about 100us. This is the ionosphere reflection at daytime of E layer, its altitude is

$h = t * \frac{c}{2} = 800 \text{ us} * 3 * \frac{10^8}{2} = 11.70\text{km}$. Furthermore, the time spread of the impulse response determine the layer's thickness by equation $T = (t_2 - t_1) * \frac{c}{2} = 120 \text{ us} * 3 * \frac{10^8}{2} = 20\text{km}$

The simulation results are consistent with the parameters in table 1.

The experimental results from UViip team (figure 13) show a ground signal at $t=0$, and other pulses at 0.84ms, 1.8ms, 3.72ms, and 5.6ms representing the reflection of the D, E, F1, F2. Altitude and thickness of ionosphere layers can be determined similarly to the above equations. The shape of channel response in the measurement matches the shape of channel response in the simulation. Hence, by adjusting the values of the simulation's variants, results of similar to the measurement can be observed.

An interesting result is shown in figure 14, where most of the pulse are disappear, and only shown are the ground wave, and pulse at $t=1\text{ms}$, and 1.7ms . This is expected, as discussed in the Literature Review section, at night (or in this case, is the sunset), the D and E layer disappear and merge into F layers. Thus, the first weak pulse would represent the reflection of D layer, and the second pulse represent reflection from the merged E and F layer.

The simulation confirmed the validation of the experiment results.

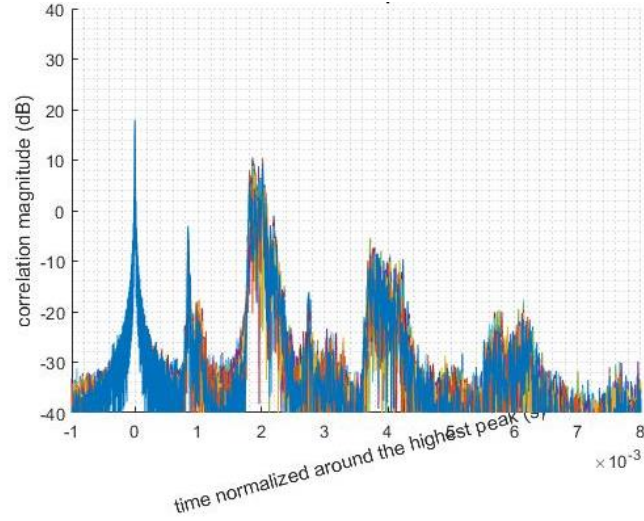


Figure 13 Experimental Ionosphere Measurement by UViip (at 22:30 on Jun19,2017)

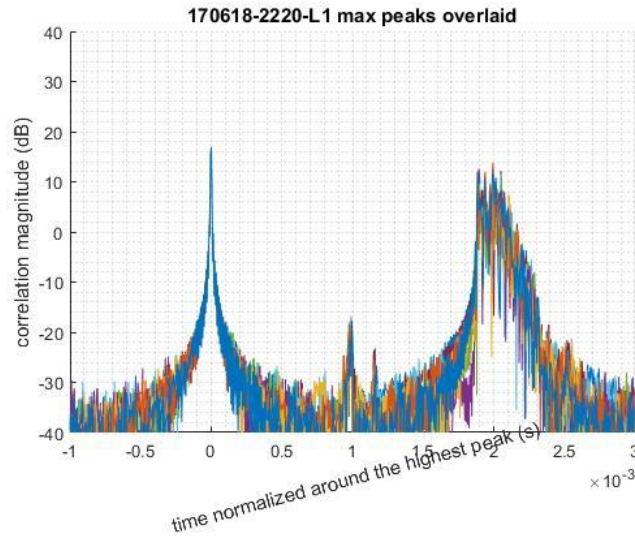


Figure 14 Experimental Ionosphere Measurement by UViip (at 22:20 on Jun18, 2017)

VII Conclusion & Recommendations

The objectives of this project is to study the propagation of HF wave through the ionosphere. The simulation result is used to compared and validated with the experimental result from the UViip Ionospheric team. The report explains an overview of the ionosphere layers and some of their properties. Then the Watterson HF channel modeling is discussed, and expand to wideband results. The derived equations are then used to be written in MATLAB code, to build a simulation of the HF Ionospheric channel. The simulation plotted the channel's time-varying frequency response, time-varying impulse response, as well as its absolute values. The simulation results are compared with the experimental results, and confirm the validation of the results.

References

- [1] Furman, W.N., Nieto, J.W.: *Understanding HF Channels Simulator Requirements in order to Reduce HF Modem Performance Measurement Variability*. In: Nordic HF Conference, pp. 6.4.1-6.4.13 (2001)
- [2] T. Yonezawa, "Theory of formation of the ionosphere", *Space Science Reviews*, vol. 5, no. 1, 1966.
- [3] I. Poole, "Radio Waves and the Ionosphere", 1999.
- [4] C. C. Watterson, J. R. Juroshek, W. D. Bensema, *Experimental Confirmation of an HF Channel Model*, IEEE Trans. On Comm. Tech., Vol. COM-18, No. 6, Dec. 1970
- [5] ITU, "HF Ionospheric Channel Simulators", CCIR Report 549-3, Recommendations and Reports of the CCIR, Annex to Vol. 3, pp. 47-58
- [6] F. Pérez Fontán and P. Mariño Espiñeira, *Modeling the wireless propagation channel*. Chichester (West Sussex, United Kingdom): Wiley, 2008.
- [7] ITU, *Recommendation 520-1 Use of High Frequency Ionospheric Channel Simulators*, Recommendations and Reports of the CCIR, Vol. III, pp. 57-58.
- [8] ITU, *HF Ionospheric Channel Simulators*, CCIR Report 549-2, Recommendations and Reports of the CCIR, Vol. III, pp. 59-67.